

Nicholas G. Paulter Jr.<sup>1</sup>

# Test Methods to Rigorously, Reproducibly, and Accurately Measure the Detection Performance of Walk-through Metal Detectors

## Reference

N. G. Paulter Jr., "Test Methods to Rigorously, Reproducibly, and Accurately Measure the Detection Performance of Walk-through Metal Detectors," *Journal of Testing and Evaluation* 48, no. 2 (March/April 2020): 1694–1711. <https://doi.org/10.1520/JTE20180220>

## ABSTRACT

Walk-through metal detectors (WTMDs) are the primary tool for the detection of concealed metal contraband and threat items on a person. They are found at almost all security checkpoint stations worldwide. It is important for security that assessing the detection performance of WTMDs is done rigorously, accurately, and reproducibly. Current standardized test methods do not provide this capability. Moreover, exhaustive testing would be prohibitively expensive and slow. Test methods, test objects, and their rationale are described here that can be used to accurately and reproducibly measure the detection performance of a WTMD while rigorously exercising its detection capability. Focused selection of the most informative test parameters reduces the time required for testing by about two orders of magnitude.

## Keywords

baseline technical performance, human motion, rectilinear scan, reproducibility, test methods, walk-through metal detector

## Introduction

Walk-through metal detectors (WTMDs) are the ubiquitous portal-type systems that are found at checkpoint security stations to search people for hidden metal objects. Although WTMDs do not provide imaging capability, depending on their design, they can provide location information for the threat. Moreover, WTMDs can find metal objects hidden inside body cavities or underneath skin folds, which advanced imaging technologies<sup>1–3</sup> typically cannot do. Therefore, it is very important to security that the WTMD functions

Manuscript received March 22, 2018; accepted for publication January 8, 2019; published online April 8, 2019. Issue published March 1, 2020.

<sup>1</sup> Material Measurement Laboratory, National Institute of Standards and Technology, 100 Bureau Dr., Mail Stop 8102, Gaithersburg, MD 20899, USA (Corresponding author), e-mail: [nicholas.paulter@nist.gov](mailto:nicholas.paulter@nist.gov), <https://orcid.org/0000-0002-9782-0894>

as it is intended and that its detection performance is accurately known. This known performance will not only help in product selection and deployment strategies but also in security modeling of multitechnology security solutions. Obtaining information on the threat item detection performance of a WTMD requires appropriate design or selection of test methods, test objects, and analysis methods, or both. These test methods should thoroughly exercise the detection performance of the WTMD. The test objects and test methods should also provide an accurate and reproducible means of measuring the WTMD detection performance. Finally, the dissemination of these tools will ensure that the detection performance of the WTMD has a common reference. The dissemination should be done through a documentary performance standard that describes the baseline technical performance requirements and associated test methods, test objects, and data analyses.

The term “baseline technical performance,” although synonymous with “minimum performance” or “minimally acceptable performance” is used here because of the confusion with equating “minimum,” in this context, to finding the smallest of some threat or with minimum being misconstrued as less than acceptable. The baseline technical performance should be a generally agreed upon performance level below which a security instrument will not be considered for use or further examination. This baseline detection performance, per National Institute of Justice (NIJ) Standard 0601.02<sup>4</sup> (which is the only published documentary performance standard for WTMDs currently available), comprises several components: test object detectability (detection sensitivity), test object transit speed, detection repeatability, through-put rate, and discrimination. The ASTM also published a standard practice for assessing the detection performance of WTMDs, which includes test object design.<sup>5</sup> Although the focus here is on thorough evaluation of the WTMD for test object detectability, both test object transit speed and detection repeatability will be naturally included in the suggested test method.

We have previously shown that nonrectilinear trajectories that emulate human motion affect the detectability of test objects presented to a WTMD.<sup>6</sup> We have also shown that test object orientation and portal entry location affect the detectability of the test object. These parameters must be considered in developing a method for evaluating the performance of a WTMD. Because human size is quite variable, it may not be sufficient to limit the number of portal entry locations for testing a WTMD even if nonrectilinear trajectories are used that are supposed to emulate certain types of motion, such as wrist sway or head bob. For example, wrist sway may occur for about quarter of the area of the portal depending on the size of a person. To ensure confidence in assessing the performance of a WTMD, object detectability maps of the entire portal area may need to be acquired using nonrectilinear trajectories. Furthermore, if test object speed through the portal and several different test objects are also considered, then the entire test space is large and can take thousands of hours to complete:

$$t_{test} = \frac{1}{4} N_{obj-orient} N_{trj} \sum_{i=1}^M t_{map,sp_i} \quad (1)$$

where  $t_{test}$  is the total test time; the factor 1/4 represents that only 1/4 of the portal area needs to be scanned for any nonrectilinear trajectory;  $t_{map,sp_i}$  is the time to perform an object detectability map at each  $i$ th speed, up to  $M$  speeds;  $N_{obj-orient}$  is the number of test object orientation pairs; and  $N_{trj}$  is the number of nonrectilinear trajectories (per previous research<sup>6</sup> there are ten unique trajectory types,  $N_{trj} = 10$ ). There are eight test objects, per the NIJ Standard (Std) 0601.02, with a different number of orientations for each test object: three orientations for one test object and six orientations for seven test objects so that  $N_{obj-orient} = 45$ . The orientations considered here are limited to the orthogonal orientations that provide a unique presentation to the WTMD. The current NIJ WTMD standard lists four speeds, 0.2 m/s, 0.5 m/s, 1.0 m/s, and 2.0 m/s. However, based on the nonrectilinear trajectories, the test object may be moving forward but also swinging backward, so the lowest speed of 0.2 m/s is not accurate. A lower speed of 0.02 m/s would more accurately represent this situation. Based on the likely use of a bandpass filter for the detection alarm circuit, which would limit low-frequency signals caused by extremely low speeds through the portal and would limit high-frequency signals caused by unrealistic high speeds through the portal, three nominal speeds are sufficient, 0.05 m/s, 0.5 m/s, and 2 m/s. Using these speeds,  $t_{map,sp_i}$  can be estimated: for a nominal scan speed of 2 m/s,  $t_{map,sp_1} \approx 10$  h; for a 0.5-m/s nominal scan speed,  $t_{map,sp_2} \approx 14$  h; and for

a nominal 0.05-m/s scan speed,  $t_{map,sp_3} \approx 54$  h, where each map is the result of 20 scans per entry point location with a spatial resolution of 5 cm. These times per map include an approximate 5 s delay between each scan to allow the response of the WTMD to the test object to relax and time to reposition the horizontal and vertical position after each set of 20 scans/entry point location. This scheme would represent a thorough testing of test object detectability, test object transit speed, and detection repeatability. These testing requirements result in  $t_{test} = 8,775$  h (about 1,097 eight-hour shifts). Although all this testing can be automated, these long test times would eliminate availability of the test instrumentation. Therefore, we would like to establish test methods that can be used to accurately measure the baseline acceptable detection performance of a WTMD without requiring thousands of hours of test time.

The orientation of the test object, as used in this document, is relative to that of the Cartesian coordinate system of the WTMD, in which the WTMD height is along the  $z$ -axis (vertical direction), its width along the  $x$ -axis (horizontal direction), and its depth along the  $y$ -axis. The  $y$ -axis is the direction through the portal of the WTMD. The orientation of the magnetic fields generated by the WTMD is different throughout the volume of the WTMD. Consequently, the local orientation of the test object relative to the WTMD-generated magnetic fields will vary as the test object passes through the portal, so WTMD geometry is used for the reference for the test object orientation and not the WTMD magnetic field.

Previous studies on WTMD testing have been reported wherein the trajectory was varied but not examined or controlled explicitly.<sup>7,8</sup> A recent study<sup>9</sup> on the evaluation of WTMDs at security checkpoints also has been performed, where the authors focused on the overall performance of the security process, including factors unrelated to WTMD detection performance. This study focuses on the testing necessary to thoroughly assess the threat detection performance of WTMDs. This study addresses current WTMD designs and not the newer ones being considered<sup>10</sup> that exploit the magnetic polarizability tensor.<sup>11</sup> Current, commercially available and fielded WTMD designs do not use the magnetic polarizability tensor in threat detection, therefore, the development of test methods to evaluate this capability would be premature and is not considered here.

Metal detection technology has been used for other applications, and it is worthwhile to mention these here. One important application is detection of buried landmines<sup>12-14</sup> and unexploded ordnance (UXO).<sup>15-18</sup> In these cases, often inductance spectroscopy or other inductive methods are used to gain more information on the possible threat because of the ubiquity of the clutter.

## Experimental Studies

Different testing parameters will be evaluated for their necessity, range, or both by examining the response of a WTMD in the context of a baseline technical requirement. The National Institute of Standards and Technology metal detector measurement system was used for these studies.<sup>19</sup> This measurement system comprises a platform for mounting the WTMD, a computer-controlled Cartesian robot for moving the test object through the portal of the WTMD, automated data acquisition, and a set of different test objects. The data acquisition software allows collection of the set of detection signal values that are obtained from each scan of the test object through the portal of the WTMD. The signal value is the analog or digital output signal provided by the WTMD that represents the detection response of the WTMD to the test object. The maximum, minimum, and average detection signal values are determined for each scan and their statistics (average, standard deviation) are stored. Because the detection signal values include values taken when the test object is outside the portal volume, only those detection signal values that are within the portal volume of the WTMD are used to compute the statistics of the maximum, minimum, and average detection signal values. The term “portal volume” used here is the height of the portal by the width of the portal by the spacing between panels. Portal volume defines the space over which tests will be performed and compared and is not intended to rigorously define the volume of space in which a metal object can be detected, which may extend beyond the portal volume. There were 324 unique entry point locations per map, with a horizontal and vertical increment of about 50 mm between entry point locations. The horizontal width of the scan area was approximately 400 mm (9 unique horizontal locations) and the vertical height of the scan area was approximately

1,750 mm (36 unique vertical locations). Each entry point location was scanned 20 times (10 forward scans and ten reverse scans), resulting in a total of 6,480 scans/map. The detailed results presented here are for two models of WTMD, which will be called WTMD1 and WTMD2, each with a given set of detection sensitivity settings. The detection sensitivity settings of the WTMDs were set arbitrarily so as not to reflect settings used in an actual security application. The exemplars used in this study were a steel (UNS G41400) handgun, zinc handgun (UNS Z35530), aluminum (UNS A95052) knife, and nonferromagnetic stainless steel (UNS S30400) knife. The dimensions and tolerances for these test objects can be found in the work by Sheen, McMakin, and Hall.<sup>1</sup>

There are several test time conditions that affect test object detectability. These are (1) test object scan type (rectilinear versus nonrectilinear) (see “Necessity of Nonrectilinear Scans”), (2) test object speed through the portal (see “Text Object Speed”), (3) test object orientation as it passes through the portal (see “Test Object and Its Orientation”), (4) number and type of test objects (see “Test Object and Its Orientation”), (5) number of portal entry locations tested, and (6) the number of repeated measurements. This work addresses (1) through (4). The purpose here is to determine if it is possible for each of (1) through (4) that a limited set of values, ideally one, can be found that would sufficiently exercise the WTMD to demonstrate its detection performance. Each of (1) through (4) are addressed independently of each other. For each of (1), (2), and (3), a set of maximum, median, mean, and minimum detection signal values are obtained that correspond to the range of values used in each of (1), (2), and (3). Condition (4) is addressed based on electromagnetic material properties and their effect on detectability.

#### NECESSITY OF NONRECTILINEAR SCANS

The first step in developing WTMD performance test methods is to determine if rectilinear scans can be used in lieu of nonrectilinear scans. The idea here is that, instead of pushing a test object through the portal at various but fixed number of locations and for the set of nonrectilinear trajectories, an object detectability map for the portal using rectilinear scans could be used to ascertain WTMD performance. As previously mentioned, a set of entry point locations for the nonrectilinear scans may not be sufficient and a nonrectilinear map may be necessary. Therefore, being able to determine if nonrectilinear scans are essential to WTMD performance assessment is paramount to designing a test protocol.

The requirement for replacing nonrectilinear scans with rectilinear scans is that the detection signal values from the nonrectilinear trajectory are a subset of detection signal values from the map, that is,

$$S_{max,map} > S_{max,traj} \quad (2)$$

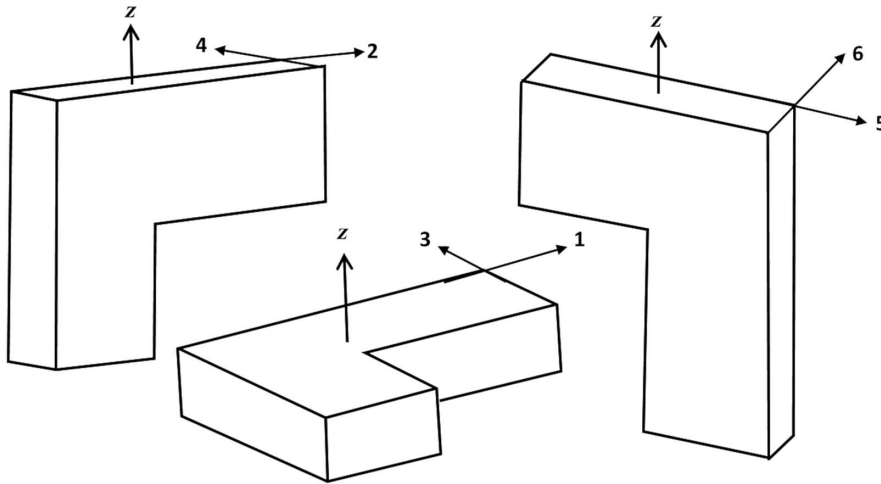
and

$$S_{min,map} < S_{min,traj} \quad (3)$$

where  $S_{max,map}$  is the maximum detection signal value from the rectilinear mapping of the test object detectability,  $S_{min,map}$  is the minimum detection signal value from the mapping,  $S_{max,traj}$  is the maximum detection signal value obtained from the nonrectilinear trajectory being examined, and  $S_{min,traj}$  is the minimum detection signal value from the nonrectilinear trajectory being examined. The detection signal is the electrical signal that becomes the basis for the generation of an alarm (typically a visible light or an audible sound). If the detection signal exceeds a preset threshold, the alarm is activated. Examples of detection signals are shown in [Table 1](#).

The nonrectilinear scans considered here emulate the type of motion expected from the human body, and include locations such as the head, wrist, and foot (see [Table 2](#)). The motion of these body parts comprises vertical, lateral (side-to-side), and anterior-posterior (front to back) components. [Table 2](#) provides nominal values for these motions as well as the standard deviation for a sample population, which represents observations of 440 different walking sequences from 115 different persons of both genders and ages ranging from 18 years to 60 years, with at least two walking sequences per person.<sup>20,21</sup> The information in [Table 2](#) was used to identify mathematical formulas that represent the observed motion,<sup>6</sup> which are the cycloid and Lemniscate of Bernoulli.

**FIG. 1** Orientations of handgun exemplar. The arrow depicts the direction of the exemplar during testing, which is along the y-axis. For example, Orientation #2 corresponds to the lower right orientation with a trajectory collinear with Arrow 2. The vertical axis is labeled with z, which is the direction parallel with the height of the WTMD portal.



### Evaluation at a Single Point in the WTMD for a Given Rectilinear Scan

The first step in determining if a rectilinear scan map can be used instead of fixed-point nonrectilinear trajectories is to acquire and compare  $S_{max,map}$ ,  $S_{min,map}$ ,  $S_{max,traj}$  and  $S_{min,traj}$ . The “wrist” trajectory (nonrectilinear) with a steel handgun exemplar in Orientation 1 (see [fig. 1](#)) was chosen to start this examination with a  $(x, z)$  entry point location of about (300 mm, 300 mm). The results of this test using WTMD1 gave  $S_{max,traj} = 0.519 \pm 0.036$  V and  $S_{min,traj} = 0.114 \pm 0.058$  V. A local rectilinear scan detectability map that encompasses the space visited by the wrist trajectory is given in [Table 1](#). The maximum detection signal in [Table 1](#) is 0.805 V, and the minimum value is 0.092 V. This table shows that, for the entry point location of  $(x, z) = (300 \text{ mm}, 300 \text{ mm})$  and for the steel handgun exemplar in Orientation 1, the requirements of equations (2) and (3) are met. This means that the local rectilinear scan map (as shown by the data in [Table 1](#)) can replace a single nonrectilinear scan centered in the middle of the map at  $(x, z) = (300 \text{ mm}, 300 \text{ mm})$ .

**TABLE 1**

Measured maximum and minimum detection signals from WTMD1 for a rectilinear trajectory

Portal Entry Point Location $(x, z)$ , mm		
Maximum Detection Signal, V		
Minimum Detection Signal, V		
(270, 255)	(300, 255)	(330, 255)
0.514 ± 0.036	0.529 ± 0.016	0.583 ± 0.014
0.119 ± 0.045	0.148 ± 0.043	0.174 ± 0.014
(270, 300)	(300, 300)	(330, 300)
0.471 ± 0.020	0.615 ± 0.031	0.805 ± 0.016
0.125 ± 0.034	0.162 ± 0.044	0.174 ± 0.015
(270, 345)	(300, 345)	(330, 345)
0.379 ± 0.014	0.471 ± 0.042	0.616 ± 0.044
0.092 ± 0.019	0.110 ± 0.031	0.124 ± 0.071

*Note:* The portal entry point locations are indicated in parentheses, and the 1- $\sigma$  standard deviation is shown.

## Evaluation of Object Detectability over Area of the WTMD Portal for a Given Rectilinear Scan

To determine if the entry point location affects whether the local map, centered on a given entry point location, can replace the nonrectilinear scan centered at the same entry point location requires performing scans similar to what was described in the section “Evaluation at a Single Point in the WTMD for a Given Rectilinear Scan,” but over the entire portal of the WTMD. To do this, nonrectilinear scans were performed at the locations shown in **Table 2** and the results compared to a complete-portal-area object detectability map (see **figs. 2** and **3**) using rectilinear scans with 5-cm spatial resolution. These data show that the extrema of the nonrectilinear scans are a subset of the extrema of the rectilinear scans.

### Object Detectability over the Portal Area of the WTMD for a Given Rectilinear Scan

The trajectory of the nonrectilinear scan described in “Evaluation of Object Detectability over Area of the WTMD Portal for a Given Rectilinear Scan,” the wrist trajectory, had the greatest displacement from the entry point location compared with all the nonrectilinear trajectories shown in **Table 3**. These nonrectilinear trajectories, as they move the test object through their respective volumes, probe the path-specific responsivity of the WTMD to that test object. The wrist trajectory probes the largest volume because that trajectory has the greatest displacement in both the horizontal and vertical directions compared with the other trajectories. Consequently, there is no physical reason why the extrema of detection signal values for the other-than-the-wrist nonrectilinear trajectories should not be contained within the extrema of detection signal values for the rectilinear scan map or for the nonrectilinear wrist scan trajectory. Consequently, because the wrist nonrectilinear scan can be replaced by a rectilinear scan map, it is possible to accurately and reproducibly represent the detection capability of the WTMD for a given test object and its orientation traveling at a given speed through the WTMD portal by

**TABLE 2**

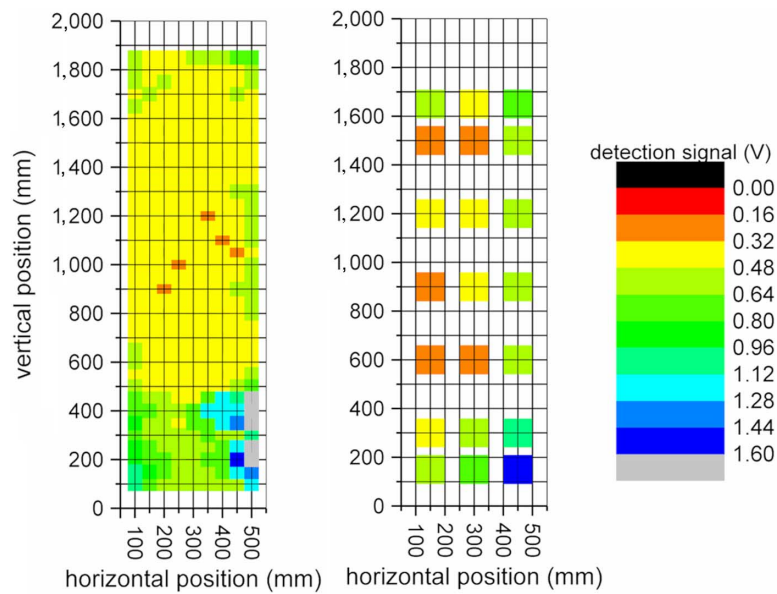
Measured maximum and minimum detection signals for WTMD1 for the wrist trajectory

	Portal Entry Point Location (x, z), mm	
	Maximum Detection Signal, V	
	Minimum Detection Signal, V	
(150, 150)	(300, 150)	(450, 150)
0.558 ± 0.004	0.768 ± 0.014	1.544 ± 0.568
0.111 ± 0.031	0.165 ± 0.005	0.488 ± 0.331
(150, 300)	(300, 300)	(450, 300)
0.367 ± 0.055	0.519 ± 0.036	1.038 ± 0.163
0.090 ± 0.008	0.114 ± 0.058	0.142 ± 0.077
(150, 600)	(300, 600)	(450, 600)
0.285 ± 0.009	0.313 ± 0.012	0.574 ± 0.004
0.063 ± 0.012	0.077 ± 0.010	0.117 ± 0.008
(150, 900)	(300, 900)	(450, 900)
0.297 ± 0.040	0.374 ± 0.003	0.631 ± 0.036
0.076 ± 0.038	0.077 ± 0.022	0.072 ± 0.030
(150, 1,200)	(300, 1,200)	(450, 1,200)
0.341 ± 0.012	0.247 ± 0.041	0.512 ± 0.004
0.074 ± 0.010	0.044 ± 0.032	0.116 ± 0.012
(150, 1,500)	(300, 1,500)	(450, 1,500)
0.413 ± 0.004	0.297 ± 0.019	0.564 ± 0.017
0.0865 ± 0.012	0.085 ± 0.004	0.099 ± 0.004
(150, 1,650)	(300, 1,650)	(450, 1,650)
0.526 ± 0.012	0.379 ± 0.014	0.714 ± 0.068
0.106 ± 0.005	0.124 ± 0.005	0.112 ± 0.006

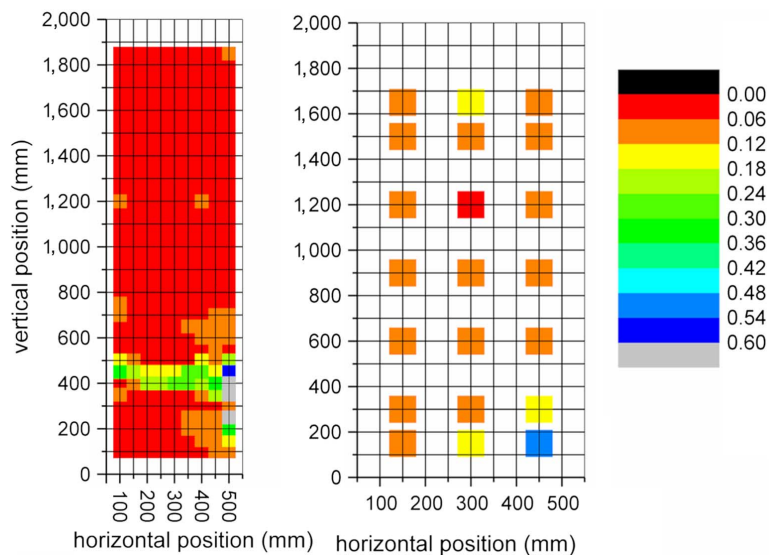
Note: The portal entry point locations are indicated in parenthesis, and the 1- $\sigma$  standard deviation is shown.

**FIG. 2**

Maximum detection signals from WTMD1 for the steel handgun in Orientation 1 moving at a speed of about 0.05 m/s. Left plot shows a dense rectilinear scan. The right plot shows a sparse wrist trajectory scan centered at indicated locations (see Table 2).

**FIG. 3**

Minimum detection signals from WTMD1 for steel handgun in Orientation 1 moving at a speed of about 0.05 m/s. Left plot shows a dense rectilinear scan. The right plot shows a sparse wrist trajectory scan centered at indicated locations (see Table 2).



one rectilinear detectability scan map of the WTMD for the same given test object, its orientation, and at the same given speed. This would reduce  $t_{test}$  to about 3,510 h (reduction from ten each 1/4 scan maps to one full scan map).

### TEST OBJECT SPEED

The localized scan speed will affect the dwell time at any particular position within the WTMD detection volume, and this may impact whether a particular trajectory's path renders the test object more detectable or not.

**TABLE 3**Magnitude of motion (mm) body part, population mean  $\pm$  standard deviation (mm)<sup>6</sup>

Body part	Anterior-posterior	Lateral	Vertical
Center of the head	16.9 $\pm$ 7.8	38.5 $\pm$ 17.8	47.0 $\pm$ 11.9
Center of the clavicle	24.7 $\pm$ 7.4	30.5 $\pm$ 9.5	46.9 $\pm$ 11.4
Left shoulder	36.8 $\pm$ 12.9	32.7 $\pm$ 10.5	51.5 $\pm$ 14.2
Left elbow	181.0 $\pm$ 49.2	66.7 $\pm$ 20.7	46.9 $\pm$ 13.7
Left wrist	402.5 $\pm$ 95.1	62.4 $\pm$ 34.8	119.2 $\pm$ 44.0
Right shoulder	37.8 $\pm$ 11.7	32.1 $\pm$ 10.5	51.2 $\pm$ 13.4
Right elbow	163.1 $\pm$ 51.4	60.9 $\pm$ 19.1	47.7 $\pm$ 13.54
Right wrist	365.3 $\pm$ 110.5	52.1 $\pm$ 29.0	106.1 $\pm$ 38.2
Center of pelvis	34.1 $\pm$ 7.7	27.9 $\pm$ 8.4	46.9 $\pm$ 11.5
Left hip joint	43.1 $\pm$ 11.4	29.7 $\pm$ 7.6	48.7 $\pm$ 11.1
Left knee	331.2 $\pm$ 36.4	37.7 $\pm$ 16.0	85.6 $\pm$ 14.7
Left ankle	685.5 $\pm$ 64.9	38.3 $\pm$ 12.8	157.1 $\pm$ 18.4
Right hip joint	40.6 $\pm$ 9.1	29.8 $\pm$ 7.4	49.6 $\pm$ 11.3
Right knee	329.0 $\pm$ 34.9	37.0 $\pm$ 16.0	83.7 $\pm$ 14.9
Right ankle	683.5 $\pm$ 63.8	38.5 $\pm$ 13.7	157.9 $\pm$ 18.0

The localized scan speed is the result of the forward motion plus the sway of the emulated body part, wherein this localized scan speed may range from almost 0 m/s to twice the speed of the forward motion. The scan maps of the detection signal maxima for rectilinear scans with speeds of nominally 0.5 m/s and 2.0 m/s for the steel handgun in Orientation 1 are shown in figures 4 and 5.

**FIG. 4**

Maximum detection signal from WTMD1 for steel handgun in Orientation 1 moving a speed of about 0.5 m/s.

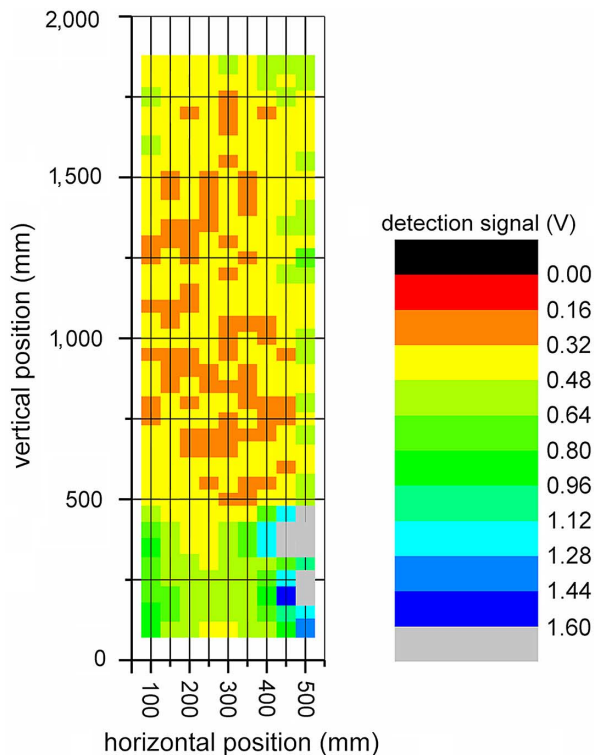
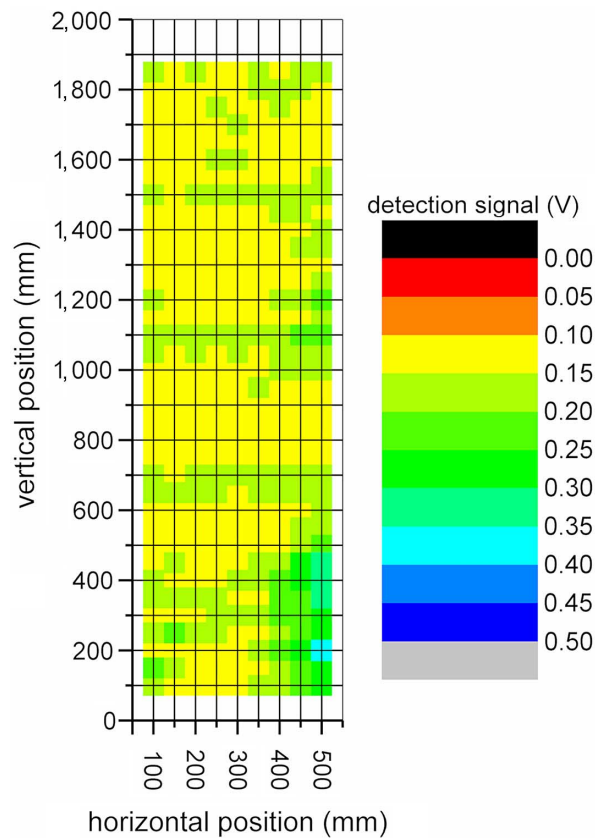


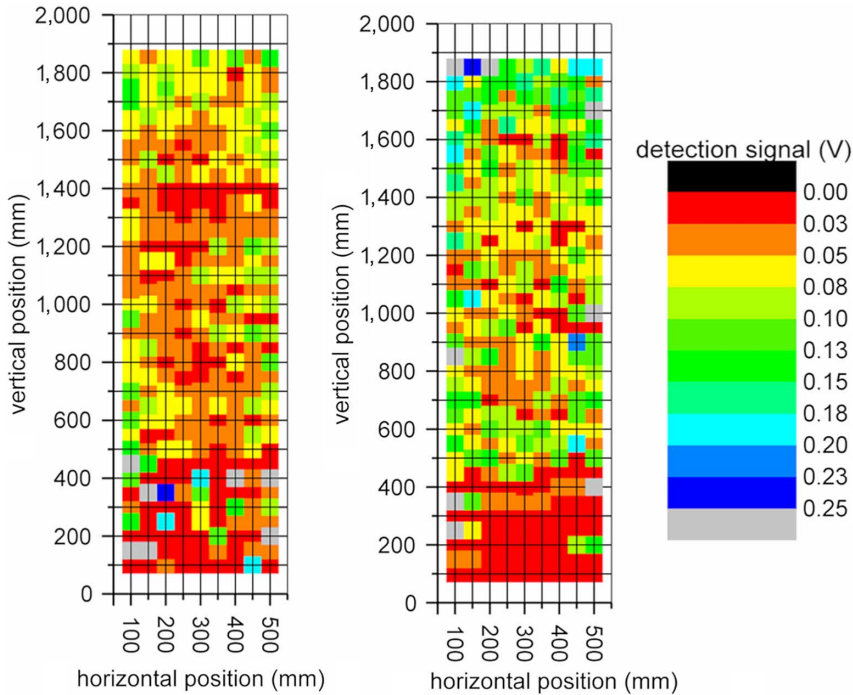
**FIG. 5**

Maximum detection signal from WTMD1 for steel handgun in Orientation 1 moving a speed of about 2.0 m/s.



The scan maps (see [figs. 4 and 5](#)) of the detection signal maxima for 0.5 m/s and 2.0 m/s rectilinear scans of the steel handgun in Orientation 1 show that the object detectability is consistent but not identical for the different transient speeds examined. The detection signal minima are not shown because they were the same value as the detection signal maxima for the nominal scan speeds of 0.5 m/s and the 2.0 m/s. This is because the data output capability of the WTMD is slow, resulting in a 25 points/scan for the 0.05 m/s scan, 3 points for the 0.5 m/s scan, and 1 point for the 2.0 m/s scan. However, only those values corresponding to the object passing through the portal volume contribute to the determination of the extrema of the detection signal values. Accordingly, the number of points in computing the detection signal extrema was restricted: for the 0.05-m/s scan, 15 points/scan were used; for the 0.5-m/s scan, 1 point was used; and for the 2.0-m/s scan, 1 point was used as the restriction was not applied. The detection signal is significantly less for the nominal 2.0-m/s scan than the 0.05-m/s and 0.5-m/s scans because the higher speed transits through the WTMD portal by the test object creates detection signals that either (a) have bandwidths near the frequency limit of the detection circuitry of the WTMD or (b) are too fast to be acquired from the readout electronics of and computer interface to the WTMD. To understand which process contributed to the difference between the low-speed and high-speed scans, 20 measurements each were taken at the nominal scan speeds of 0.01 m/s, 0.2 m/s, 1.0 m/s, and 2.0 m/s at  $(x, z) = (300, 750)$ . The results (mean and standard deviation) are  $0.197 \pm 0.007$  V at 0.05 m/s,  $0.307 \pm 0.009$  V at 0.1 m/s,  $0.309 \pm 0.010$  V at 1.0 m/s, and  $0.295 \pm 0.017$  V at 2.0 m/s for the stainless steel knife exemplar at Orientation 6. For these data, the signal is nominally constant for scan speeds corresponding to normal traffic flow and decreases significantly (about 35 %) for slower scan speeds and slightly (5 %) for higher speeds. Also, the ratio of the standard deviation to mean is about two times greater for the highest scan speed than for the other scan speeds while the standard

**FIG. 6** Standard uncertainty for detection signal values from WTMD1. The left plot is for measurements performed using a scan speed of nominally 0.05 m/s, and the right plot is for a scan speed of nominally 0.5 m/s.



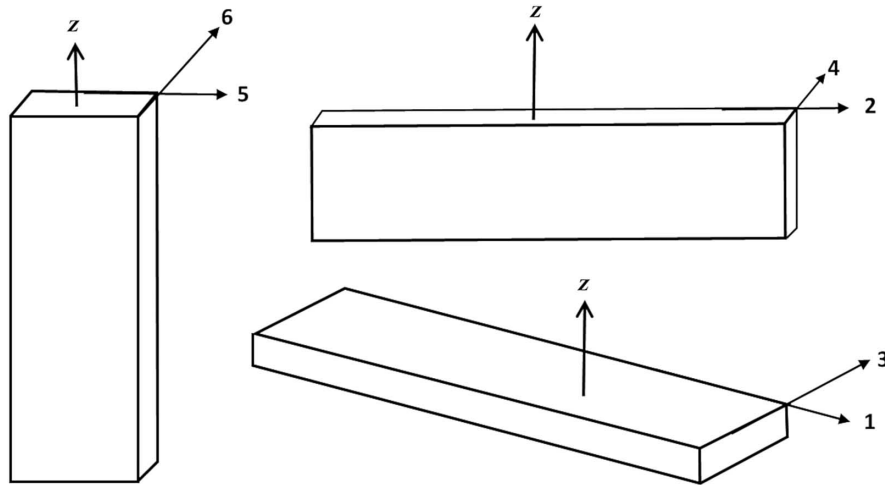
deviation increases with scan speed. These results imply that the reduced amplitude in the acquired detection signal values at the 2.0 m/s scan are caused by the readout electronics/computer interface.

The speed data show that the local relative detectability of the test object with its orientation for the WTMD is similar, if measurement uncertainties are considered (see [fig. 6](#)), for speeds less than 2.0 m/s. Consequently, only one speed is necessary to assess WTMD object detectability performance. The typical transit speed through the WTMD portal, based on observation, is about 0.5 m/s. In typical operation of a WTMD at a security checkpoint, an officer/operator is present to limit excessive speed through the WTMD. Consequently, to cover higher transit speeds than is typical, a scan speed of approximately 1 m/s is suggested for field and laboratory testing. To ensure that the detection circuitry does have an appropriate bandwidth, however, several scans at other speeds at entry point locations that provide small detection signals should be performed. Using only one speed for the testing of the detection sensitivity (object detectability) performance of the WTMD will reduce  $t_{test}$  to about 495 h (one full map at 1 m/s instead of three 1/4 maps each at three different scan speeds, wherein the 1 m/s map takes about 11 h to complete).

## Test Object and Its Orientation

The orientation of the test object will affect its detectability. The number of orientations for a given test object that are necessary to represent that test object has not been previously addressed. Examples of test object orientation for a knife exemplar are shown in [figure 7](#). Although this assessment can be performed using electromagnetic field modeling, the complex nature of the magnetic fields of a WTMD make actual experimental assessments more general and applicable than modeling. Measurements are more general and applicable than modeling to the goal of establishing baseline technical performance requirements while providing a thorough and accurate

**FIG. 7** Knife exemplar and its orientations for WTMD testing. The arrow depicts the direction of the exemplar during testing, which is along the y axis. For example, Orientation #3 corresponds to the lower right orientation with a trajectory collinear with Arrow 3. The vertical axis is labeled with z, which is the direction parallel with the height of the WTMD portal.



assessment of the performance of a WTMD. To determine if one orientation can be used to establish a baseline technical performance for object detectability, all of the test objects given in NIJ Std 0601.02 were considered. These test objects are grouped into three size categories: large object, consisting of steel (UNS G41400), zinc (UNS Z35550), and aluminum (UNS A96961) handgun exemplars; medium object, consisting of steel (UNS G41300) and aluminum (UNS A95052) knife exemplars; and small object consisting of a steel (UNS G10180) handcuff key exemplar, a nonferromagnetic steel (UNS S30400) knife exemplar, and a steel (UNS G41400) #2 screwdriver bit exemplar. Not all of these exemplars are necessary for testing the detection performance of a WTMD, as will now be discussed, but were included because of nontechnical reasons to include exemplars representing items found in use in the NIJ Std 0601.02.

Of the statistics collected (mean, median, maximum, and minimum) for the detection signal, the selection of test object orientation is based on the minimum detection signal, as this is signal that should be greater than the alarm threshold if an object of a given size or greater is to be detected. More specifically, it is the minimum of the set of maximum detection signals, or maximum lower bound (MLB), for each orientation that should be greater than the alarm threshold. Anything lower than this MLB may result in nuisance alarms and anything greater may result in missed alarms. The test object orientation that provides the least MLB is chosen for WTMD testing purposes.

The aluminum and zinc hand exemplars both are constructed of material that have a relative magnetic permeability of about 1. Because zinc has an electrical conductivity less than that of aluminum and the aluminum and zinc handgun exemplars have the same dimensions, the zinc handgun exemplar will be harder to detect than the aluminum handgun exemplar. Consequently, detection performance of the WTMD does not have to be tested for the aluminum handgun exemplar if it has been tested for the zinc handgun exemplar. The handcuff key and #2-Phillips-screwdriver bit exemplars are both constructed of ferromagnetic metals. The electrical conductivity of the screwdriver bit and handcuff key exemplar are about the same, but the magnetic permeability of the handcuff key exemplar is about four times greater than that of the screwdriver bit exemplar.<sup>22</sup> Although the handcuff key and screwdriver bit exemplars do not have the same dimensions, the difference in magnetic permeability would make the screwdriver bit exemplar less detectable than handcuff key exemplar, which was verified by simulations of the interaction of a simple circular magnetic field with the exemplars.<sup>22</sup> Consequently, only the screwdriver bit needs to be used for testing the detection performance of a WTMD. Using these physics-based arguments, the

number of test objects and orientations can be reduced by a factor of 12 (six orientations each for the aluminum handgun and handcuff key exemplars). This will reduce  $t_{test}$  by about 132 h to give  $t_{test} = 363$  h.

**Figure 8** shows the object detectability maps of WTMD1 using Setting1 for the six orientations of the steel handgun, and **Table 4** shows the statistics of those maximum detection signal values shown in **figure 8**. Setting1 is a global sensitivity setting, that is, a not zone-specific sensitivity setting, which will be given a relative value of nominally 0.90 of Setting2. These data show that Orientations 2 and 5 are the orientations of the steel handgun exemplar that render it the least detectable (see boldface entries in **Table 4**). This is consistent with expectation based on the magnetic field distribution, exemplar geometry and orientation, and the size and magnetic permeability of the test object. The steel handgun exemplar is a notched rectangular parallelepiped (looking like an L-shaped extrusion), in which the parallelepiped dimensions are nominally 76 by 57 by 14 mm (length by width by thickness), and the notch dimensions are approximately 56 by 37 mm (length by width).

**Figure 9** contains the detectability maps of WTMD1 using Setting2 for the six orientations of the steel knife, and **Table 5** contains the statistics associated with those detectability maps. Setting2 is a global sensitivity setting

**FIG. 8** Detectability maps, as given by the maximum detection signal values, of WTMD1 using Setting1 for the steel handgun in different orientations (see **fig. 1**), as indicated above the graph. All maps were obtained with a scan speed of about 1 m/s.

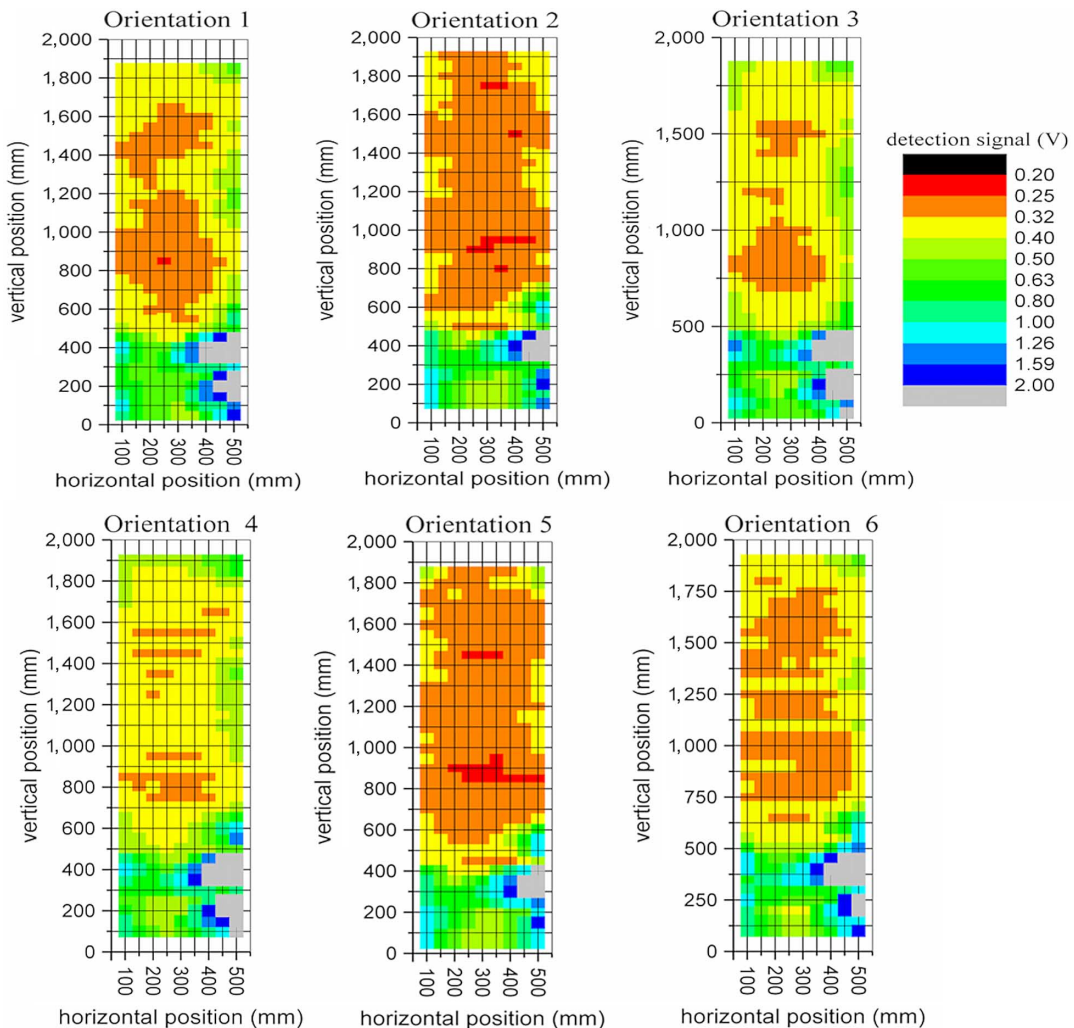


**TABLE 4**

Statistics of the maximum detection signal values from WTMD1 (as shown in **fig. 8**) for the steel handgun exemplar

Orientation	Mean, V	Standard Deviation, V	Minimum, V	Median, V	Maximum, V
1	0.553	0.698	0.251	0.345	6.335
2	0.437	0.390	0.225	0.303	3.983
3	0.595	0.772	0.271	0.369	7.186
4	0.596	0.782	0.276	0.376	7.551
5	0.439	0.406	0.232	0.295	3.963
6	0.553	0.686	0.262	0.342	7.045

**FIG. 9** Detectability maps, as given by the maximum detection signal values, of WTMD1 using Setting2 for the steel knife in different orientations (see **fig. 7**), as indicated above the graph. All maps were obtained with a scan speed of about 1 m/s.

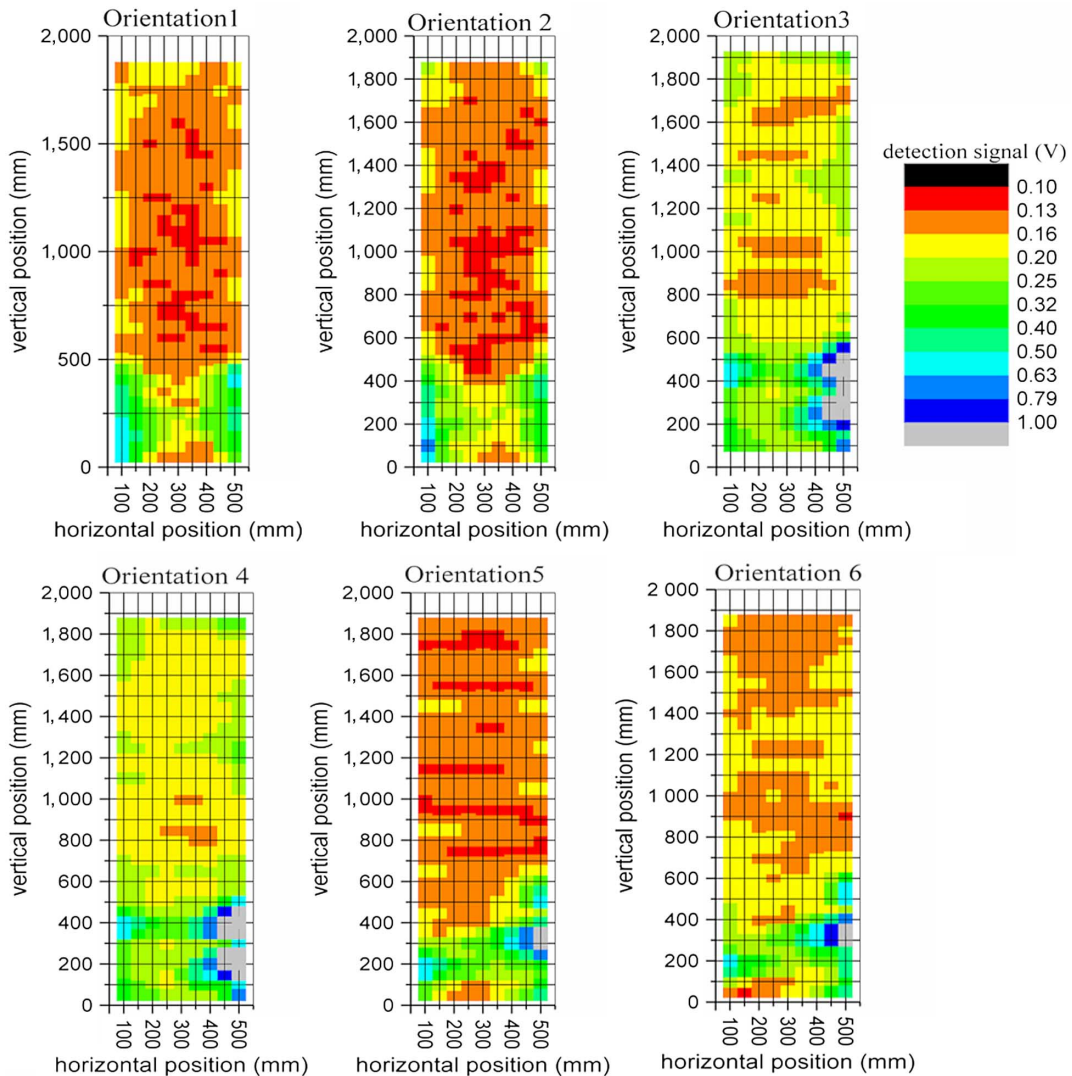


**TABLE 5**

Statistics of the maximum detection signal values from WTMD1 (as shown in [fig. 9](#)) for the steel knife exemplar

Orientation	Mean, V	Standard Deviation, V	Minimum, V	Median, V	Maximum, V
1	0.173	0.080	0.110	0.144	0.578
2	0.167	0.075	0.105	0.141	0.632
3	0.261	0.276	0.131	0.189	2.639
4	0.268	0.281	0.150	0.195	2.543
5	0.171	0.082	0.108	0.141	0.714
6	0.197	0.130	0.123	0.161	1.429

with a given relative value of 1.00. These data show that Orientations 1, 2, and 5 are the orientations of the steel knife exemplar that render it the least detectable (see boldface entries in [Table 5](#)). This is consistent with expectation based on the magnetic field distribution, exemplar geometry and orientation, and the size and magnetic permeability of the test object. The steel knife exemplar is a parallelepiped, in which the parallelepiped dimensions are nominally 76 by 19 by 1.6 mm (length by width by thickness).

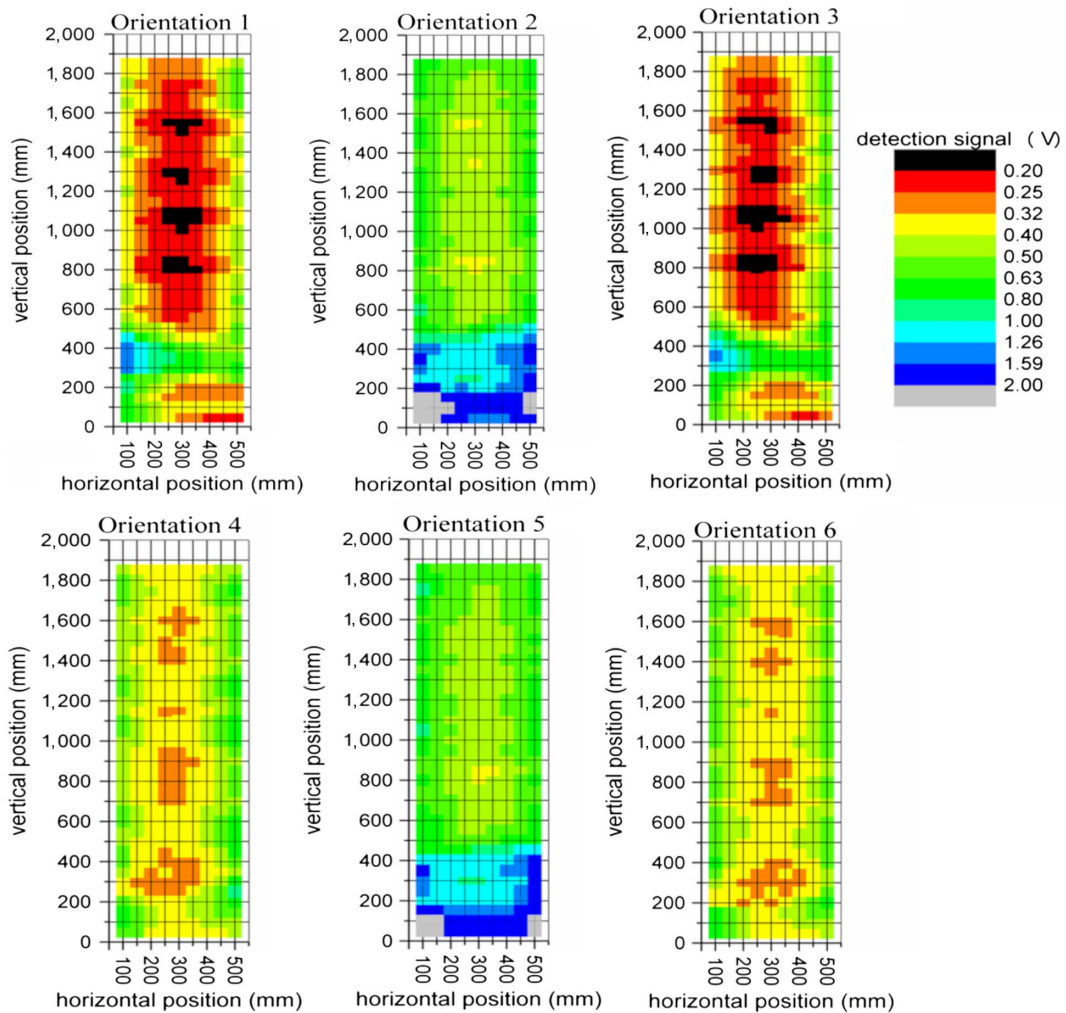
[Figure 10](#) contains the detectability maps of WTMD2 for the six orientations of the stainless steel knife, and [Table 6](#) contains the statistics associated with those detectability maps. WTMD2 was used here to include details from a different model WTMD. These data show that Orientations 1 and 3 are the orientations of the stainless steel knife exemplar that render it the least detectable (see boldface entries in [Table 6](#)). This is consistent with expectation based on the magnetic field distribution, exemplar geometry and orientation, and the size and magnetic permeability of the test object. The stainless steel knife exemplar has the same dimensions as the steel knife exemplar.

[Table 7](#) contains information from WTMD1 Setting3, WTMD2 Setting5, and a third WTMD, designated WTMD3. The values in [Table 7](#) were normalized to range from 0 to 1. The detection sensitivity settings for WTMD1 and WTMD2 that were used to obtain the data shown in [Table 1](#) are different than those settings used for the data elsewhere presented. The trends shown in detail in [figures 8–10](#) are consistent with that shown in [Table 7](#), namely that the least and most detectable orientations are similar for the different WTMDs. Setting3 is a global sensitivity setting with a given relative value of nominally 0.65 Setting2. Setting5 of WTMD2 is approximately 0.90 Setting4.

These data, as shown in [figures 8–10](#) and [Tables 4–7](#), show that there is an orientation that provides minimal detectability throughout the volume of the portal. As previously mentioned, the detection sensitivity of the different zones of the WTMD used to generate these data was adjusted to purposefully give a variable object detectability throughout the portal. Although these settings may not represent those used in an actual security application, the result that a given test object has an orientation that renders it minimally detectable does not change. Furthermore, studies on other WTMD models verify that this observation regarding a minimally detectable test object orientation is applicable to other WTMD models. Therefore, the threat detection performance of the WTMD can be thoroughly tested using that orientation of the threat object exemplar that provides its minimum detectability. This reduces the number of orientations to one per exemplar. Because six exemplars, one each constructed of ferromagnetic and nonferromagnetic metals for each of the three object size categories, are required to test the object detectability of the WTMD,  $t_{test}$  can be reduced to about 66 h (6 exemplars, 11 h/map, and 1 map/exemplar).

The effect of rotation of the exemplar about an axis has not been examined in this study, although it was shown to be a significant issue for hand-held and hand-worn metal detector testing,<sup>22,23</sup> and in both cases, resulted in documentary standards for these products that use spherical test objects.<sup>24,25</sup> Those studies show that rotation of less than 10° from the ideal alignment (which is where the Cartesian axes of the test objects are parallel to the Cartesian axes of the magnetic fields) during product testing may cause the hand-held metal detector to appear to detect an object of a smaller size classification than it actually can detect. The rotation of the exemplar

**FIG. 10** Detectability maps, as given by the maximum detection signal values, of WTMD2 Setting4 for the stainless steel knife in different orientations (see [fig. 7](#)), as indicated above the graph. All maps were obtained with a scan speed of about 1 m/s.



may not be a significant issue with the WTMD because of the complexity of the magnetic field and, consequently, the uniformity of object detectability throughout the WTMD detection volume. However, rotation about the axes was not rigorously controlled or measured in this study and may have been up to  $10^\circ$  from the ideal alignment.

**TABLE 6**

Statistics of the maximum detection signal values from WTMD2 (see [fig. 10](#)) for the stainless steel knife exemplar

Orientation	Mean, V	Standard Deviation, V	Minimum, V	Median, V	Maximum, V
1	0.359	0.188	0.168	0.304	1.460
2	0.763	0.462	0.371	0.567	2.825
3	0.368	0.179	0.172	0.310	1.317
4	0.414	0.100	0.291	0.385	0.838
5	0.752	0.433	0.390	0.573	2.897
6	0.410	0.091	0.287	0.382	0.759

TABLE 7

Maximum detection signal values for WTMD1, WTMD2, and WTMD3 for different test objects

Orientation	1	2	3	4	5	6
WTMD1 Setting3						
Steel Handgun	3.5	1.0	6.7	10.0	2.6	7.5
Zinc Handgun	1.8	10.0	1.8	1.0	9.2	1.0
Aluminum Handgun	1.0	10.0	1.9	1.9	10.0	1.9
Steel Knife	3.6	1.0	8.7	10.0	2.3	3.6
Aluminum Knife	5.0	10.0	4.1	1.0	8.5	1.2
WTMD2						
Steel Handgun	8.2	1.7	10.0	7.6	1.0	5.3
Zinc Handgun	1.2	9.2	1.0	4.8	10.0	5.3
Aluminum Handgun	1.9	9.6	1.4	1.0	10.0	5.1
Steel Knife	7.7	2.3	10.0	8.4	1.0	4.7
Aluminum Knife	1.0	10.0	1.0	2.3	9.6	2.5
SS Knife	2.6	10.0	1.0	2.0	9.6	2.2
#2 Screwdriver Bit	10.0	1.0	3.8			
Handcuff Key	7.1	2.6	10.0	8.9	1.0	4.4
WTMD3						
Steel Handgun		1.0	10.0	8.9		
Zinc Handgun	1.0	10.0	1.0	7.4	10.0	8.7
Aluminum Handgun	1.0	10.0	1.0	7.8	10.0	9.3
Steel Knife	8.5	2.5	10.0	6.0	1.0	3.8

Note: These values were normalized to range from 1 to 10.

Rotations of 90° will affect the signal, of course, as this amount of rotation constitutes a different orientation. Rotation may introduce a measurement uncertainty that should be included in a reported test object detectability statement and, in this case, additional measurements may be required that would increase  $t_{test}$ . Consequently, the effect of test object rotation on its detectability should be examined and this, along with a strategy for including this effect in a reasonable and thorough WTMD detection performance process if needed, will be the subject of a subsequent study. Moreover, such an examination may suggest different test object designs.

## Summary

Based on the tests and analysis done here, the test object set can be reduced to six: two each for the three different detection performance size classes. These test objects are, using NIJ Std 601.02 as a reference, the steel handgun and the zinc handgun for large size, the steel knife and the aluminum knife for the medium size, and for the small size, the #2 Philips screwdriver bit and the nonferromagnetic stainless steel knife. The orientation that provides the minimum object detectability depends on the magnetic properties of the test object. For ferromagnetic test objects, Orientation 2 was the least detectable orientation. That orientation corresponds to the largest surface of the test object being parallel to the  $y$ - $z$  plane and the long axis of the test object parallel to the  $y$ -axis, where the  $y$ -axis is direction passing through the portal of the WTMD and the  $z$ -axis is the vertical axis. For nonferromagnetic test objects, Orientation 1 or 3 provided the least detectable orientation. The signal levels are very similar for these two orientations, and within measurement uncertainty. Orientation 3, on average, provides a less detectable orientation than Orientation 1. For Orientation 3, the largest surface of the test object is parallel to the  $x$ - $y$  plane, and the long axis of the test object is parallel to the  $x$ -axis.

Thorough and reproducible measurements of the threat detection performance of WTMDs are important for selecting the correct WTMD model and its settings for any given security application. A thorough measurement process that includes different trajectories to emulate of human motion, different test object orientations,

and different speeds of the test object through the portal of the WTMD was estimated to require almost 9,000 h of test time using a robotic system. The results given here show that one trajectory type, one speed, and one orientation each for six different threat object exemplars are sufficient to accurately and reproducibly measure the threat detection performance of a WTMD. This reduces the required time for threat object detectability tests to about 66 h (a reduction in test time by a factor of about 130).

## References

1. D. M. Sheen, D. L. McMakin, and T. E. Hall, "Three-Dimensional Millimeter-Wave Imaging for Concealed Weapon Detection," *IEEE Transactions on Microwave Theory and Techniques* 49, no. 9 (September 2001): 1581–1592, <https://doi.org/10.1109/22.942570>
2. S. F. Hallowell, "Screening People for Illicit Substances: A Survey of Current Portal Technology," *Talanta* 54, no. 3 (May 2001): 447–458, [https://doi.org/10.1016/S0039-9140\(00\)00543-9](https://doi.org/10.1016/S0039-9140(00)00543-9)
3. B. Elias, *Airport Body Scanners: The Role of Advanced Imaging Technology in Airline Passenger Screening*, CRS Report for Congress R42750 (Washington, DC: Congressional Research Service, 2012).
4. *Walk-through Metal Detectors for Use in Concealed Weapon and Contraband Detection*, NIJ Standard 0601.02 (Washington, DC: United States Department of Justice, 2003).
5. *Standard Practice for Evaluation of Metallic Weapons Detectors for Controlled Access Search and Screening*, ASTM F1468–04a (2018) (West Conshohocken, PA: ASTM International, 2018). <https://doi.org/10.1520/F1468-04AR18>
6. D. R. Larson, N. G. Paulter, and N. F. Troje, "Walk-through Metal Detector Testing and the Need to Emulate Natural Body Motion," *Journal of Testing and Evaluation* 47, no. 1 (2019): 627–639, <https://doi.org/10.1520/JTE20170342>
7. C. Nelson, V. Chaudhary, J. Edman, and P. Kantor, "Walk-through Metal Detectors for Stadium Security," in *2016 IEEE Symposium on Technologies for Homeland Security* (New York: Institute of Electrical and Electronics Engineers), 1–6, <https://doi.org/10.1109/THS.2016.7568969>
8. C. Nelson, P. Kantor, B. Nakamura, B. Ricks, R. Whytlaw, D. Egan, A. Matlin, F. Roberts, M. Tobia, and M. Young, "Experimental Designs for Testing Metal Detectors at a Large Sports Stadium," in *2015 IEEE Symposium on Technologies for Homeland Security* (New York: Institute of Electrical and Electronics Engineers), 1–7, <https://doi.org/10.1109/THS.2015.7225280>
9. J. Skorupski and P. Uchroński, "A Fuzzy Model for Evaluating Metal Detection Equipment at Airport Security Screening Checkpoints," *International Journal of Critical Infrastructure Protection* 16 (March 2017): 39–48, <https://doi.org/10.1016/j.ijcip.2016.11.001>
10. L. A. Marsh, C. Ktistis, A. Järvi, D. W. Armitage, and A. J. Peyton, "Three-Dimensional Object Location and Inversion of the Magnetic Polarizability Tensor at a Single Frequency Using a Walk-through Metal Detector," *Measurement Science and Technology* 24, no. 4 (March 2013): 045102, <https://doi.org/10.1088/0957-0233/24/4/045102>
11. P. D. Ledger and W. R. Lionheart, "Understanding the Magnetic Polarizability Tensor," *IEEE Transactions on Magnetics* 52, no. 5 (May 2016): 6201216, <https://doi.org/10.1109/TMAG.2015.2507169>
12. P. Gao, L. Collins, P. M. Garber, N. Geng, and L. Carin, "Classification of Landmine-like Metal Targets Using Wideband Electromagnetic Induction," *IEEE Transactions on Geoscience and Remote Sensing* 38, no. 3 (May 2000): 1352–1361, <https://doi.org/10.1109/36.843029>
13. I. J. Won, D. A. Keiswetter, and T. H. Bell, "Electromagnetic Induction Spectroscopy for Clearing Landmines," *IEEE Transactions on Geoscience and Remote Sensing* 39, no. 4 (April 2001): 703–709, <https://doi.org/10.1109/36.917876>
14. W. R. Scott, "Broadband Array of Electromagnetic Induction Sensors for Detecting Buried Landmines," in *2008 IEEE International Geoscience and Remote Sensing Symposium* (New York: Institute of Electrical and Electronics Engineers, 2008). <https://doi.org/10.1109/IGARSS.2008.4779006>
15. T. H. Bell, B. J. Barrow, and J. T. Miller, "Subsurface Discrimination Using Electromagnetic Induction Sensors," *IEEE Transactions on Geoscience and Remote Sensing* 39, no. 6 (June 2001): 1286–1293, <https://doi.org/10.1109/36.927451>
16. J. T. Miller, T. H. Bell, J. Soukup, and D. Keiswetter, "Simple Phenomenological Models for Wideband Frequency-Domain Electromagnetic Induction," *IEEE Transactions on Geoscience and Remote Sensing* 39, no. 6 (June 2001): 1294–1298, <https://doi.org/10.1109/36.927452>
17. Y. Zhang, L. Collins, H. Yu, C. E. Baum, and L. Carin, "Sensing of Unexploded Ordnance with Magnetometer and Induction Data: Theory and Signal Processing," *IEEE Transactions on Geoscience and Remote Sensing* 41, no. 5 (May 2003): 1005–1015, <https://doi.org/10.1109/TGRS.2003.810922>
18. H. H. Nelson and J. R. McDonald, "Multisensor Towed Array Detection System for UXO Detection," *IEEE Transactions on Geoscience and Remote Sensing* 39, no. 6 (June 2001): 1139–1145, <https://doi.org/10.1109/36.927427>
19. N. G. Paulter Jr., D. R. Larson, and R. H. Palm Jr., *A Measurement System for Characterizing the Detection Performance of Metal Detectors: Design and Operation, NISTIR 6530* (Gaithersburg, MD: National Institute of Standards and Technology, 2000). <https://doi.org/10.6028/NIST.IR.6530>
20. N. F. Troje, "Decomposing Biological Motion: A Framework for Analysis and Synthesis of Human Gait Patterns," *Journal of Vision* 2, no. 2 (September 2002): 371–387, <https://doi.org/10.1167/2.5.2>

21. N. F. Troje, "Retrieving Information from Human Movement Patterns," in *Understanding Events: From Perception to Action*, T. F. Shipley and J. M. Zacks, eds. (Oxford, UK: Oxford University Press, 2008), 308–334, <https://doi.org/10.1093/acprof:oso/9780195188370.001.0001>
22. N. G. Paulter Jr., D. R. Larson, and J. A. Ely, "Test Object for Accurate and Reproducible Measurement of the Detection Response of Hand-Worn and Hand-Held Metal Detectors," *Journal of Research of the National Institute of Standards and Technology* 121 (September 2016): 401–419, <https://doi.org/10.6028/jres.121.019>
23. N. G. Paulter, D. R. Larson, and J. A. Ely, "Handheld Metal Detector Characterization Using Spherical Test Objects," *Journal of Testing and Evaluation* 48, no. 2 (March 2020): 1262–1276, <https://doi.org/10.1520/JTE20170339>
24. *Performance Standard for Hand-Worn Metal Detectors Used in Safety and Security*, ASTM F3020-16 (West Conshohocken, PA: ASTM International, 2016). <https://doi.org/10.1520/F3020-16>
25. *Standard Performance Specification for Hand-Held Metal Detectors Used in Safety and Security*, ASTM F3278-17 (West Conshohocken, PA: ASTM International, 2017). <https://doi.org/10.1520/F3278-17>